Supplementary Information:

Pairing Ru-doped NiCo-layered double hydroxides and selenide derivatives as self-supporting electrocatalyst for alkaline overall water splitting

Yuxia Wang [a], Juan Xiao [a], Tingting Huang [a], Ying Wang[a], Hui Ding [a], Qimeng Zhu[a], Guancheng Xu *[a], Li Zhang *[a,b]

a State Key Laboratory of Chemistry and Utilization of Carbon Based Energy Resources, College of Chemistry, Xinjiang University, Urumqi, 830017, Xinjiang, PR China

b College of Chemical Engineering, Xinjiang University, Urumqi, 830017, Xinjiang, PR China

*Corresponding authors. E-mail: xuguanchengxju@163.com; zhangli420@xju.edu.cn

Chemicals

All chemical reagents are utilized without purification. Nickel nitrate hexa hydrate ($Ni(NO_3)_2·6H_2O$, AR, 98%, Tianjin Yongsheng Fine Chemical Co., Ltd.), Cobalt nitrate hexahydrate($Co(NO_3)_2·6H_2O$, AR, 99.9%, Shanghai Aladdin Bioche mical Technology Co., Ltd.), Ruthenium chloride hydrate($RuCl_3.xH_2O$, 99%, Ru 3 7-40%,Beijing Yinnokai Technology Co., Ltd), Selenium powder (Se, AR, 99.9%, Shanghai Aladdin Biochemical Technology Co., Ltd.), Potassium hydroxide (KOH, AR, 85%, Tianjin Zhiyuan Chemical Reagent Co., Ltd.), commercial Pt-C (20 wt%, JM, Shanghai Hesen Electric Co., Ltd.), RuO_2 (Shanghai Hesen Electric Co., Lt d.) and NF (SHENZHEN KEJING STAR TECHNOLOGY CO., LTD. Thickness:1.6 mm).

Materials characterization.

The morphology and detailed microstructures of the final products were characterized by scanning electron microscopy (SEM) with Hitachi S-4800 scanning electron microscope and transmission electron microscopy (TEM) with FEI F30 transmission electron microscope. X-ray diffraction (XRD) patterns were recorded on a Bruker D8 advance X-ray diffractometer with Cu Kα radiation source (λ = 1.54178 Å). X-ray photoelectron spectroscopy (XPS) was performed using Thermo Fisher Scientific Escalab 250 Xi with monochromatic Al Kα at 15 kW. The Fourier transform infrared

(FTIR) spectrum was obtained using a Bruker Vertex 70 spectrophotometer within the range of 4000-400 cm^{-1}.

Electrochemical measurements

All the electrochemical tests were measured in 1.0 M KOH aqueous electrolyte with the CHI 660E electrochemical workstation. HER and OER were carried out in the three-electrode system and the two-electrode system was used to test overall water splitting performance. In this work, the graphite electrode was used as counter electrode and Hg/HgO was used as reference electrode. The area of the working electrode immersed into the electrolyte was 0.5 cm×0.5 cm.

The preparation methods of Pt-C/NF and RuO_2/NF are as follows: 0.466 mg Pt-C and 2.36 mg RuO_2 powder were dispersed in 500 μL mixed solution ($V_{ethanol}$:V_{nafion} = 490:10), respectively. Then mixed solution is ultrasonically treat ed for 1 h to form a uniform ink solution. All of the ink solution were coate don a piece of nickel foam with the area of 0.5 cm×0.5 cm, respectively, and then dried at 60 ℃ for 12 h in vacuum.

The working electrode was scanned by Cyclic Voltammetry (CV) until the signals were stabilized and then the data were collected. The Linear scanning voltammetry (LSV) was carried out at a scan rate of 5 mV s^{-1} in 1.0 M KO H and was corrected with 85% iR compensation. The potentials were calibrat ed to a reversible hydrogen electrode (RHE) according to the equation:
E (RHE) = E (Hg/HgO) + 0.098 + 0.059 pH - 85% iR (pH = 13.8, correspondin g 1.0 M KOH).

To assess the reaction kinetics, Tafel slopes were extracted from the Taf el equation: η = b log j + a b is the Tafel slope and j denotes the current density. The double layer capacitance (C_{dl}) was determined by CV curves in t he non-faradic potential region with different scan rates (60, 70, 80, 90, and 100 mV s^{-1}).The electrochemical impedance spectroscopy (EIS) measurements were conducted over a frequency range of 0.01-10^5 Hz with a 5 mV AC pote ntial perturbation. For overall water splitting, a two-electrode configuration w as adopted, andthe electrolyte of 1.0 M KOH was utilized. The stability was

evaluated via CV for 5000 cycles with a scan rate of 100 mV s^{-1} and the Chr onopotentiometry v-t methods.

The Faraday efficiencies of the H-NMO/CMO/CF-450 during the HER/OER were calculated based on the ratio of the volume of actual (V_{actual}) H_2/O_2 evo lvedto the theoretical one ($V_{theoretical}$):

$$\text{Faraday efficiency} = \frac{V_{actual}}{V_{theoretical}} \times 100\%$$

The actual volumes of generated H_2/O_2 gas were gathered using the drai nage method. The theoretical volume can be calculated by the formula:

$$V_{\text{t heoretical}} = \frac{I \cdot t \cdot V_m}{z \cdot F}$$

where I is current (A), t is time (s), V_m is molar volume of H_2/O_2 gas (23.6 L mol^{-1}, 293 K, 103.4 kPa in Urumqi, Xinjiang), F is the Faraday constant (96485 C mol^{-1}), *z* is electron number transferred per molecule (z is 2 and 4 for HER and OER, respectively).

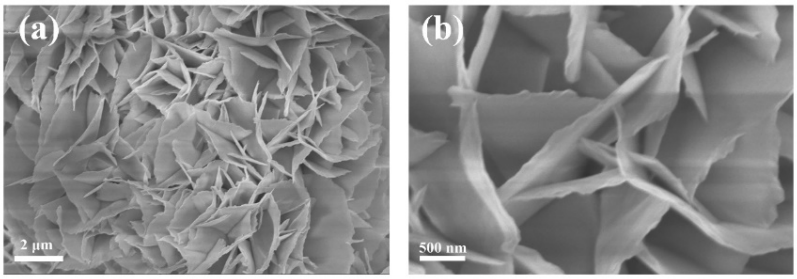

Fig. S1 SEM images of NiCo LDH/NF.

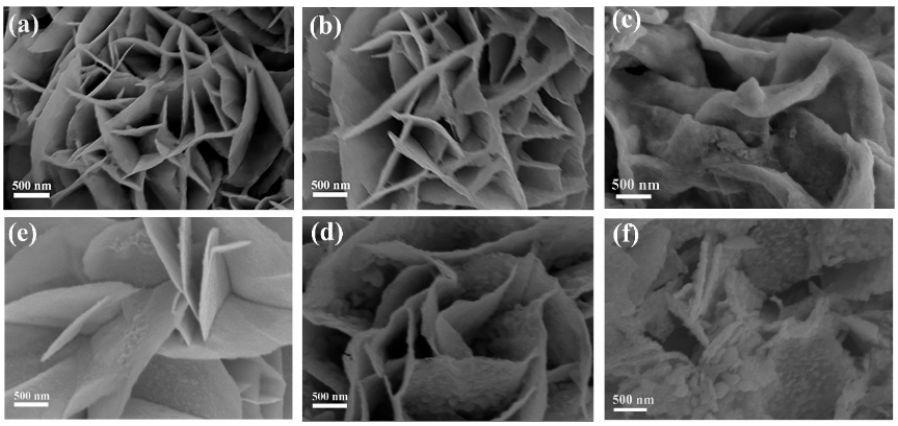

Fig. S2 SEM images of (a) Ru-NiCo LDH/NF-3, (b) Ru-NiCo LDH/NF-4, (c) Ru-NiCo LDH/NF-5, (d) Ru-$NiSe_2$/CoSe/NF-3, (e) Ru-$NiSe_2$/CoSe-4, (f) Ru-$NiSe_2$/CoSe/NF-5.

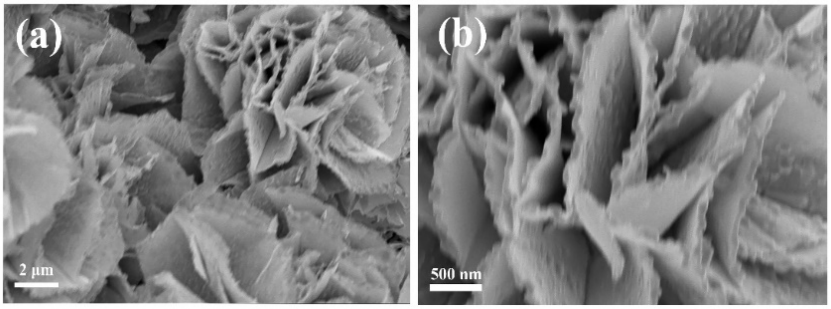

Fig. S3 SEM images of $NiSe_2$/CoSe/NF.

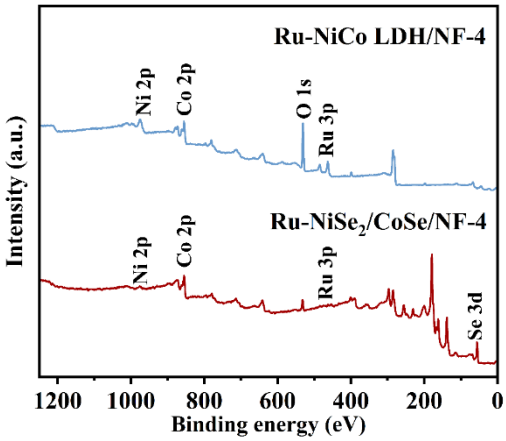

Fig. S4 XPS full spectrum of Ru-NiCo LDH/NF-4 and Ru-$NiSe_2$/CoSe/NF-4.

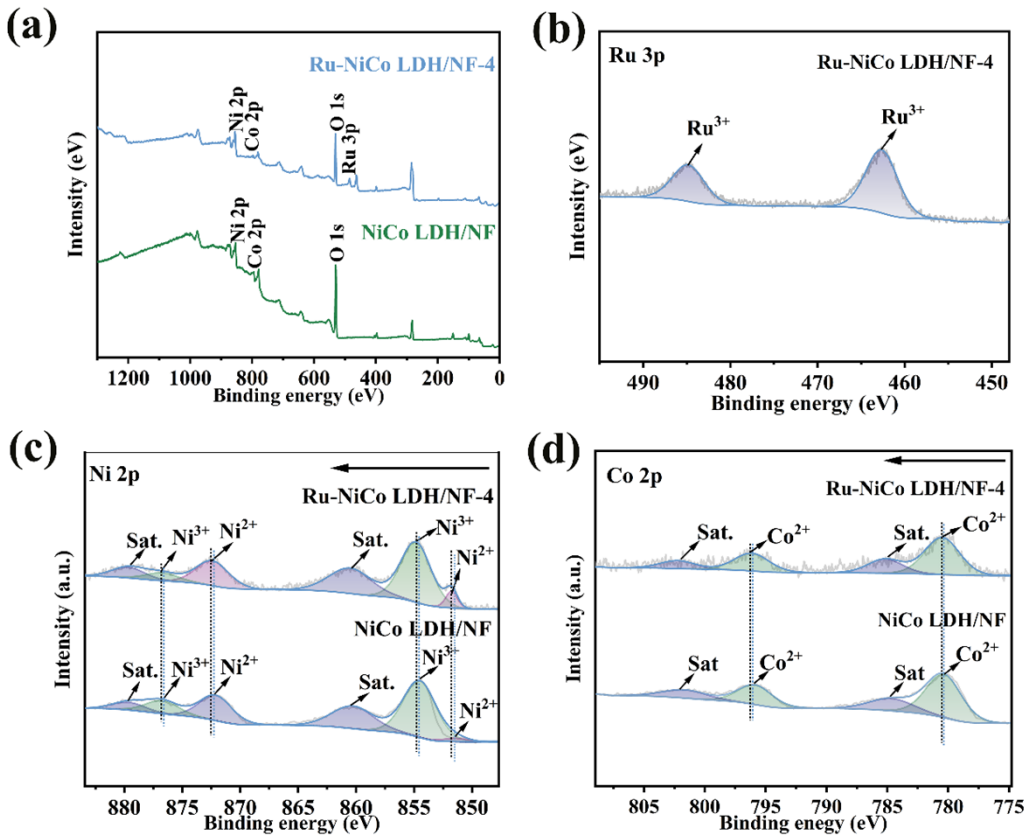

Fig. S5 XPS spectra of (a) XPS full spectrum, (b) Ru 3p, (c) Ni 2p and of Co 2p Ru-NiCo LDH/NF-4 and NiCo LDH/NF.

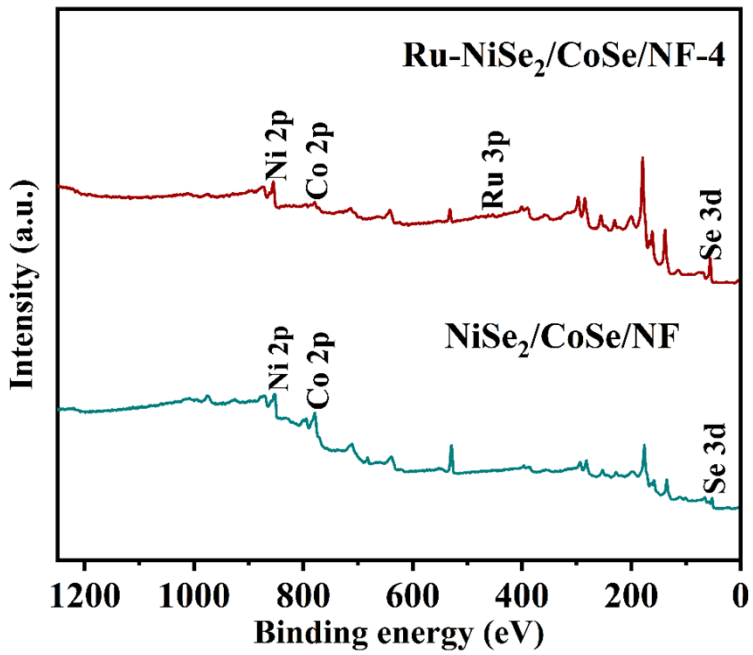

Fig. S6 XPS full spectrum of Ru-$NiSe_2$/CoSe/NF-4 and Ru-$NiSe_2$/CoSe/NF.

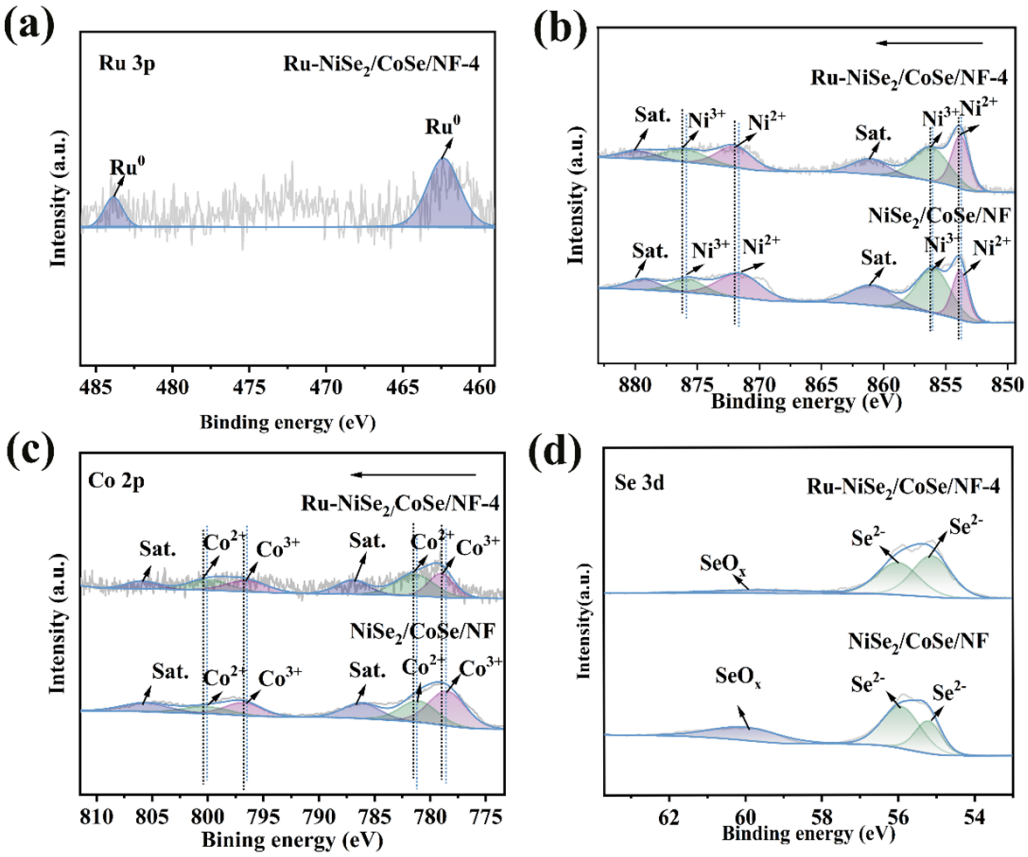

Fig. S7 XPS spectra of (a) XPS full spectrum, (b) Ni 2p, (c) Co 2p (d)Se 3d of Ru-$NiSe_2$/CoSe/NF-4 and $NiSe_2$/CoSe /NF.

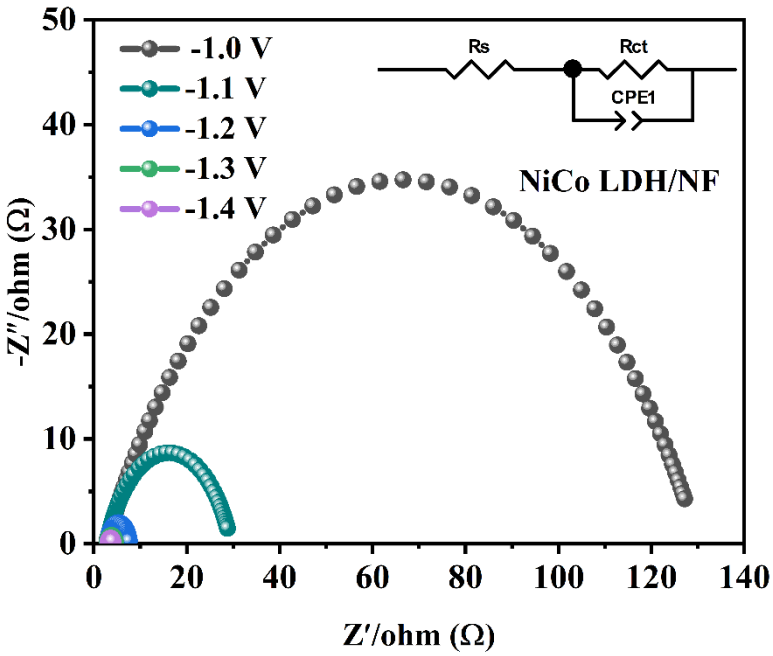

Fig. S8 Operando Nyquist of NiCo LDH/NF at various overpotentials in 1.0 M KOH.

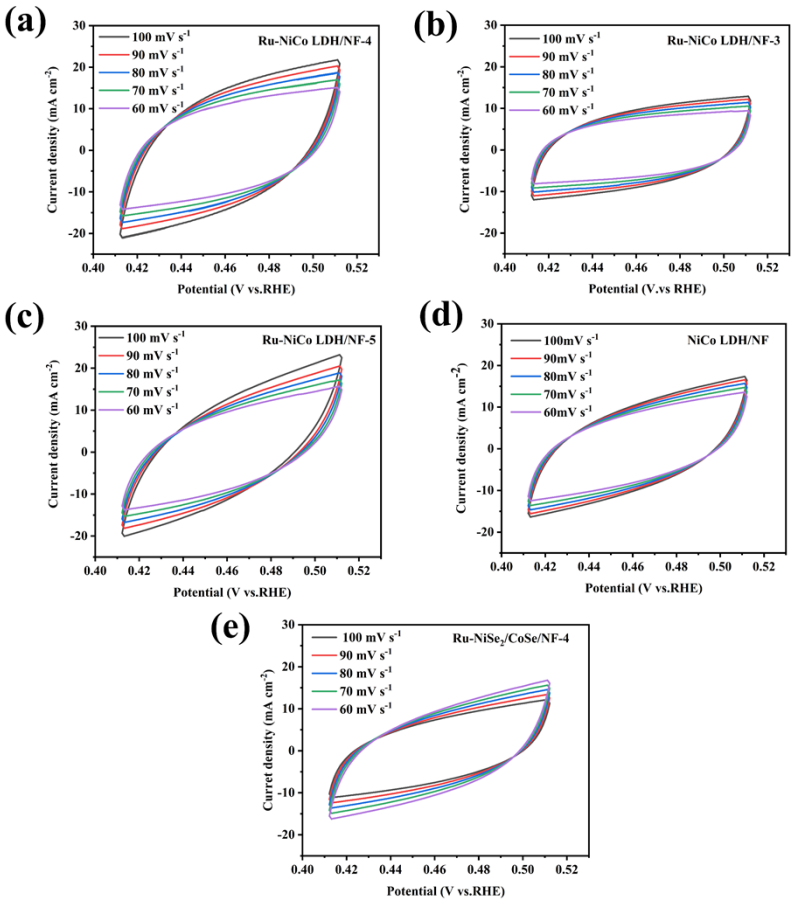

Fig. S9 CV scans of (a) NiCo LDH/NF, (b) Ru-NiCo LDH/NF-3, (c) Ru-NiCo LDH/NF-4, (c) Ru-NiCo LDH/NF-5 and Ru-$NiSe_2$/CoSe/NF-4 at various scan rate for HER.

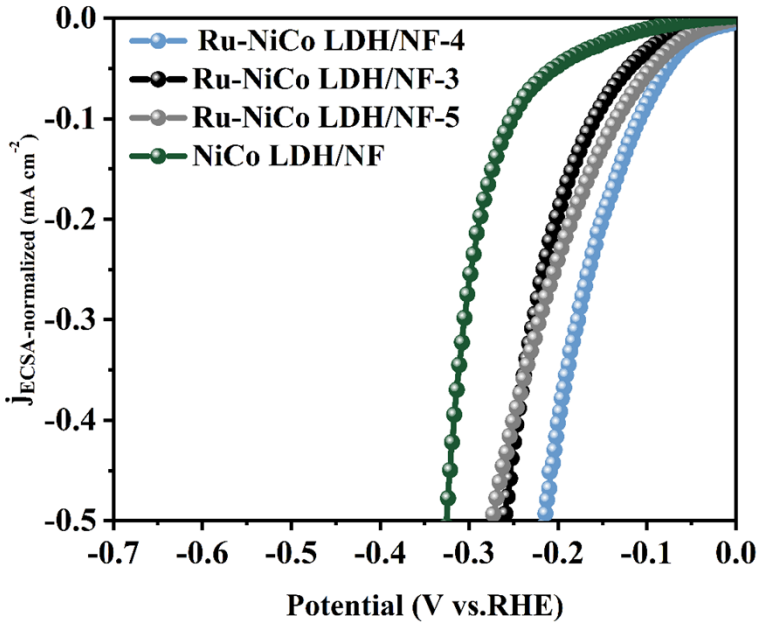

Fig. S10 ECSA normalized LSV of Ru-NiCo LDH/NF-3, Ru-NiCo LDH/NF-4, Ru-NiCo LDH/NF-5 and NiCo LDH/NF for HER.

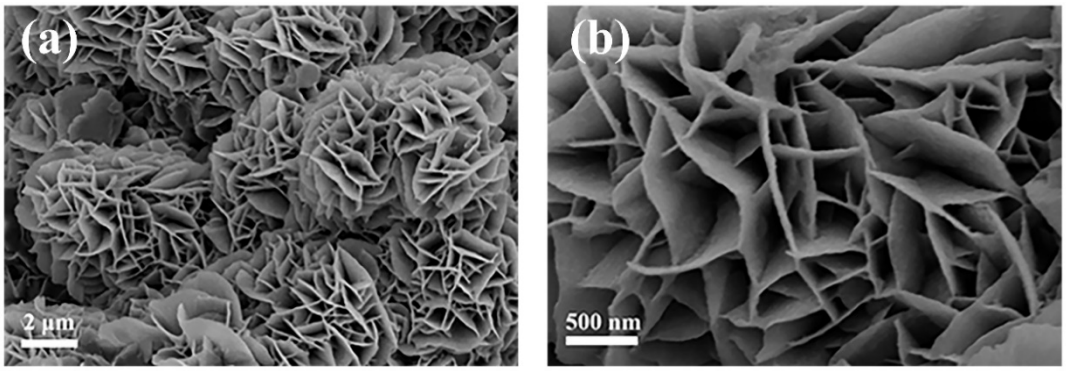

Fig. S11 (a,b) SEM after HER stability test of Ru-NiCo LDH/NF-4.

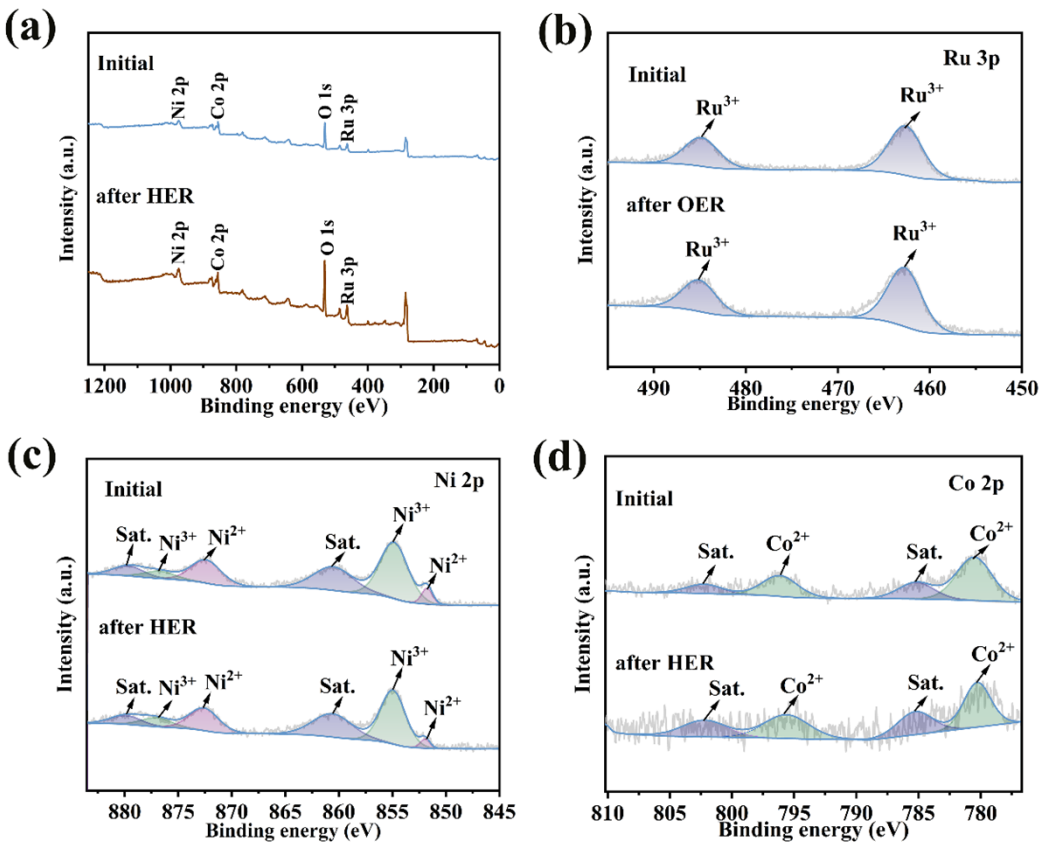

Fig. S12 XPS spectra of (a) XPS full spectrum, (b) Ru 3p, (c) Ni 2p and (d) Co 2p of Ru-NiCo LDH/NF-4 after HER stability test.

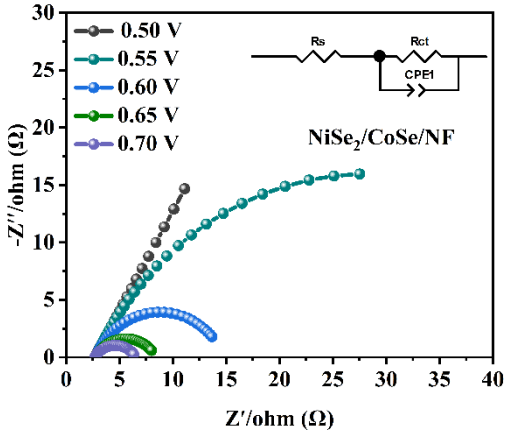

Fig. S13 Operando Nyquist of $NiSe_2$/CoSe/NF at various overpotentials in 1.0 M KOH.

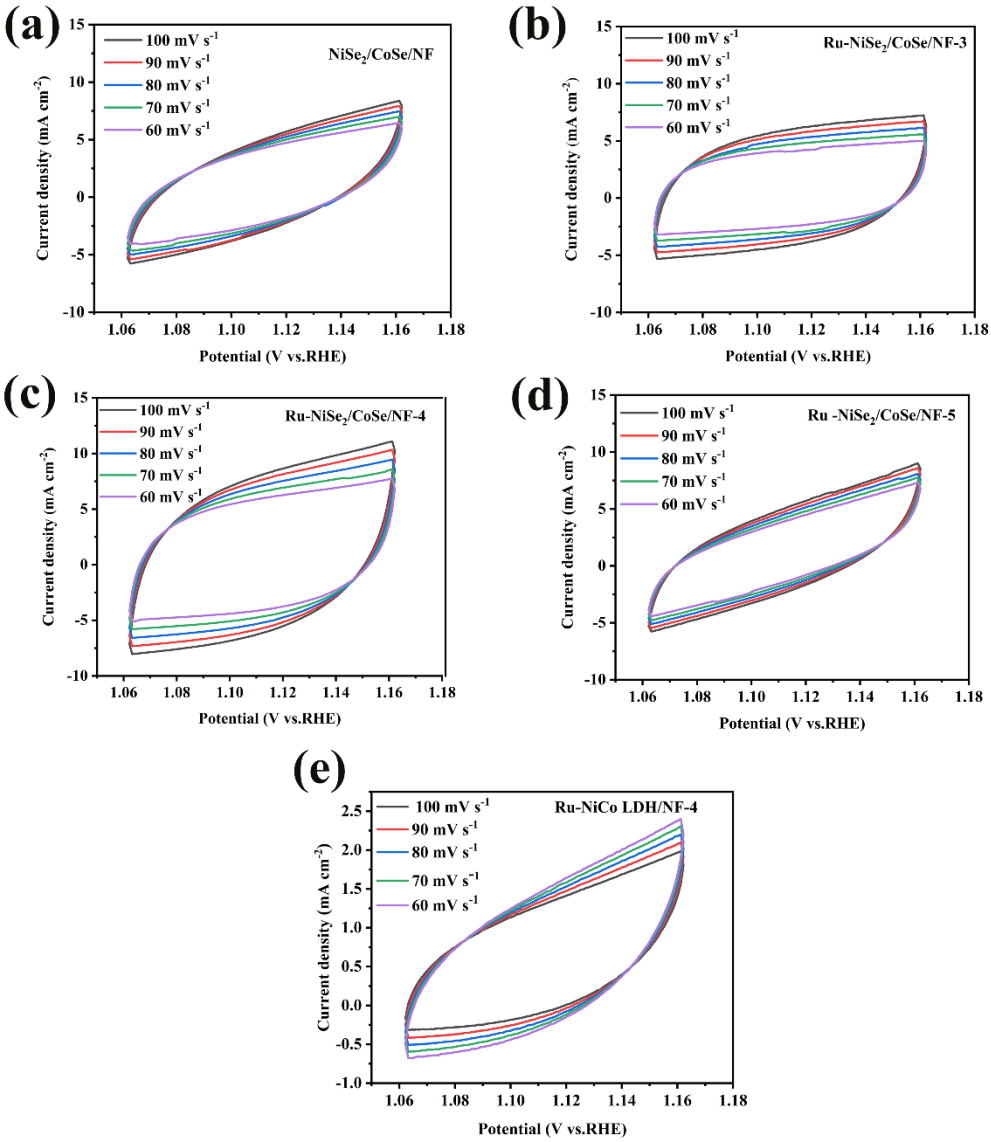

Fig. S14 CV scans of (a) $NiSe_2$/CoSe/NF, (b) Ru-$NiSe_2$/CoSe/NF-3, (c) Ru-$NiSe_2$/CoSe/NF-4, (d) Ru-$NiSe_2$/CoSe/NF-5 and (e) Ru-NiCo LDH/NF-4 at various scan rate for OER.

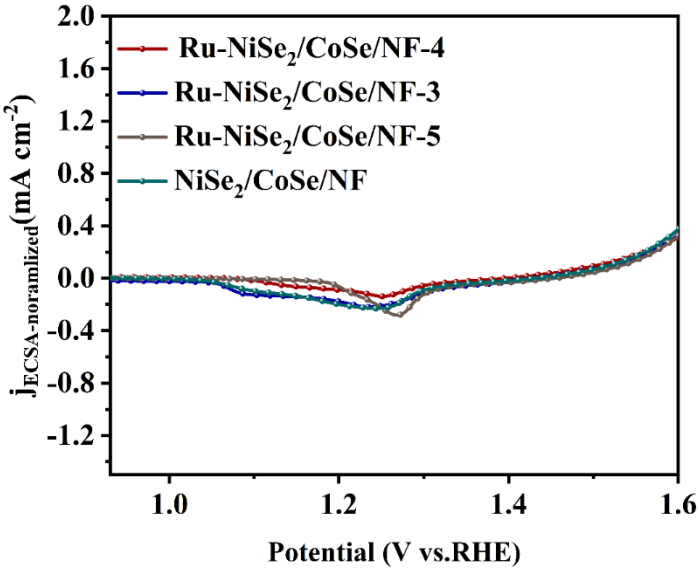

Fig. S15 ECSA normalized LSV of Ru-NiCo LDH/NF-4, Ru-NiCo LDH/NF-3, Ru-NiCo LDH/NF-5, NiCo LDH/NF for HER.

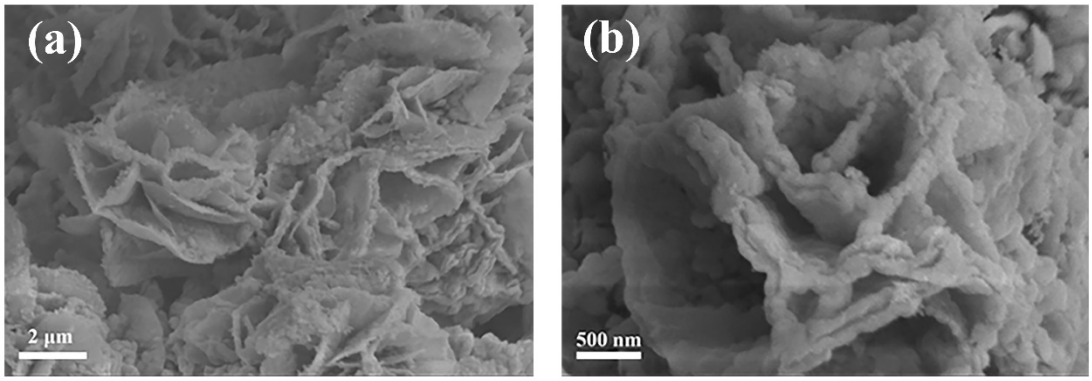

Fig. S16 (a,b) SEM after OER stability test of Ru-$NiSe_2$/CoSe/NF-4.

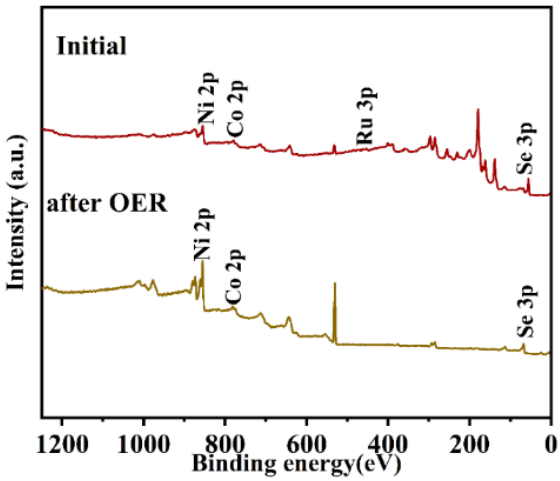

Fig. S17 XPS full spectrum after OER stability test of Ru-$NiSe_2$/CoSe/NF-4.

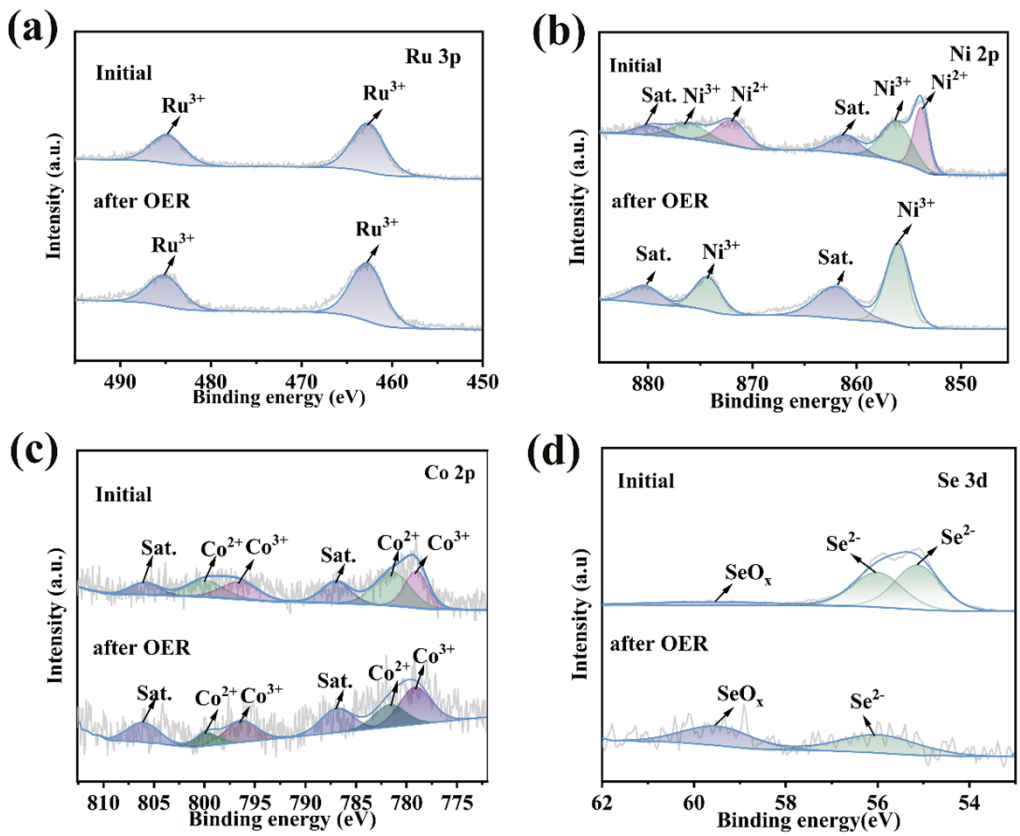

Fig. S18 XPS spectra of (a) Ru 2p, (b) Ni 2p, (c) Co 2p and (d) Se 3d of Ru-$NiSe_2$/CoSe/NF after OER stability test.

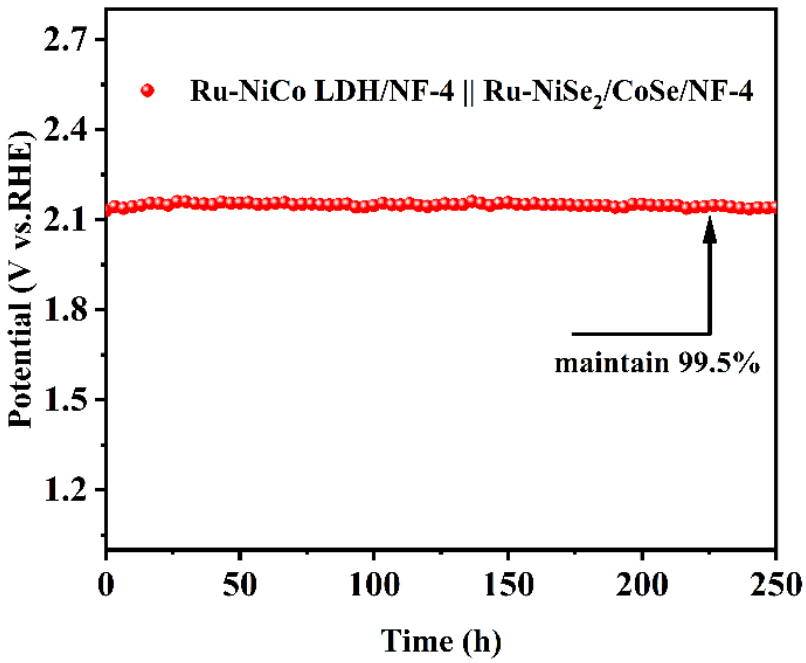

Fig. S19 chronoamperometry test of Ru-NiCo LDH/NF-4 || Ru-NiSe2/CoSe/NF-4 in 1.0 M KOH.

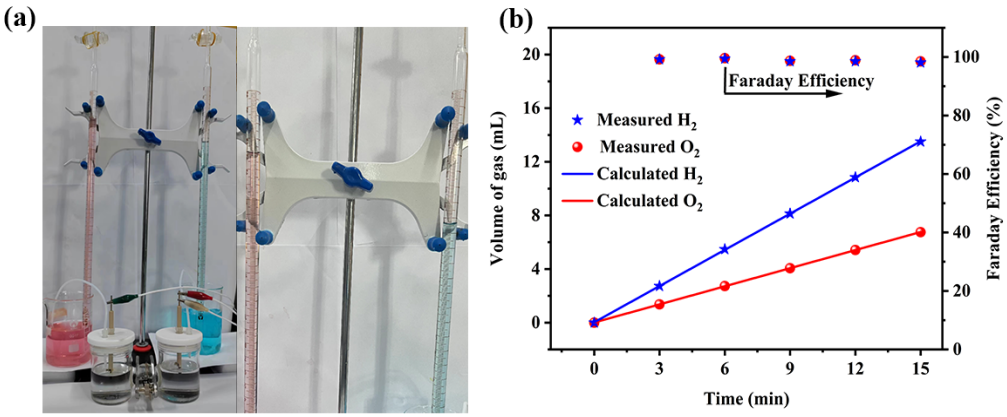

Fig. S20. (a) Photographs of the water electrolysis; (b) experimental and theoretical volumes of H_2 and O_2 gases during water splitting at a current density of 500 mA·cm^{-2} for 15 min and Faraday efficiency of the Ru-NiCo LDH/NF-4 and Ru-$NiSe_2$/CoSe/NF-4

Table S1. HER activities of the recently reported catalysts in literature (1.0 M KOH).

Catalysts	η(mV)@J(mA·cm^{-2})	Stability(h)@J(mA·cm^{-2})	Reference
Ru-NiCo LDH/NF-4	45@10	300@10	This work
H-CoS_x@NiFe LDH/NF	95@10	100@	[1]
NiFe LDH-NS@DG10	115@10	10@10	[2]
Cu_2O_S_Co_CoFe	280@100	24@200	[3]
Mo-NiS_x@NiFe LDH/NF	61.3@10	80@200	[4]
$Ni_xFe_yMo_z$ LDH	86@10	50@10	[5]
Ni_2Mo_3N/NF	59.7@10	200@15	[6]
NiFeV-LDHs/NF	125@10	15@30	[7]
Ru doped Ni(OH)$_2$/TM-0.3	135@10	15@10	[8]
Ru-CoP-2.5-NAS	52@10	50@100	[9]
Co_9S_8@NiCo LDH/NF	168@10	12@10	[10]
$Fe_{88.46}P_{9.42}$	436@10	8.6 (d) @10	[11]
2Mo/1Co	14@10	197 h@10	[12]
NF/FeNiP-CoP@NC	254@10	50 h@-0.254V	[13]

Table S2. OER activities of the recently reported catalysts in literature (1.0 M KOH).

Catalysts	η(mV)@J(mA·cm^{-2})	Stability(h)@J(mA·cm^{-2})	Reference
Ru-$NiSe_2$/CoSe/NF-4	238@10	300@10	This work
CuNi@NiSe	293@10	280@250	[14]
$FeSe_2$/NF	245@10	18@10	[15]
$Ni(CN)_2$/$NiSe_2$	270@10	10@10	[16]
Ni-Mo-Se/NF-AO	244@10	30@10	[17]
$Ni_{0.85}$Se-O/CN	240@10	48@	[18]
Fe-$NiSe_2$-25	250 @10	15@10	[19]
S-Ni_3Se_4-2	275 @10	100@50	[20]
NiFe@NiFe	241@10	100@10	[21]
FeOOH(Se)/IF	287@10	100@10	[22]
Ni–Fe–Se cages	240@10	22@5	[23]
$Fe_{88.46}P_{9.42}$	527@10	42@10	[11]
NF/FeNiP-CoP@NC	78@10	50@1.347V	[13]

Table S3. Electrolytic water splitting activities of the recently reported catalysts in literature (1.0 M KOH).

Catalysts	η(V)@J (mA·cm^{-2})	Stability (h)@J (mA·cm^{-2})	Reference
Ru-NiCo DH/NF-4||Ru-$NiSe_2$/CoSe /NF-4	1.53@10	300@10	This work
$Co_{0.9}Fe_{0.1}$-Se / NF|| $Co_{0.9}Fe_{0.1}$-Se / NF	1.55@10	36@10	[24]
P-$NiSe_2$@N-CNTs/NC|| P-$NiSe_2$@N-CNTs/NC	1.609@10	28@50	[25]
(Ni,Co)0.85Se NSAs||(Ni,Co)0.85Se	1.65@10	50@30	[26]

NSAs			
Fe@Ni3Se4/NF|| Fe@Ni3Se4/NF	1.64@50	33@50	[27]
NiSe-$Ni_{0.85}$/CP|| NiSe-$Ni_{0.85}$/CP	1.62@10	50@10	[28]
NF/FeNiP-CoP@NC|| NF/FeNiP-CoP@NC	1.478@10	50h	[13]

Reference:

1. Y. J. Lee and S.-K. Park, *Small*, 2022, **18**, 2200586.
2. Y. Jia, L. Zhang, G. Gao, H. Chen, B. Wang, J. Zhou, M. T. Soo, M. Hong, X. Yan, G. Qian, J. Zou, A. Du and X. Yao, *Adv.Mater.*, 2017, **29**, 1700017.
3. V. V. Burungale, H. Bae, M. A. Gaikwad, P. Mane, J. Heo, C. Seong, S.-H. Kang, S.-W. Ryu and J.-S. Ha, *Chem. Eng. J.*, 2024, **486**, 150175.
4. Y. Li, H. Guo, Y. Zhang, H. Zhang, J. Zhao and R. Song, *J. Mater. Chem. A*, 2022, **10**, 18989-18999.
5. A. I. Inamdar, H. S. Chavan, J. H. Seok, C. H. Lee, G. Shin, S. Park, S. Yeon, S. Cho, Y. Park, N. K. Shrestha, S. U. Lee, H. Kim and H. Im, *J. Mater. Chem. A*, 2022, **10**, 20497-20508.
6. J. Y. Zhao, Z. X. Lou, L. Y. Xue, Y. Ding, X. Li, X. Wu, Y. Liu, H. Y. Yuan, H. F. Wang, P. F. Liu, S. Dai and H. G. Yang, *J. Mater. Chem. A*, 2023, **11**, 7256-7263.
7. K. N. Dinh, P. Zheng, Z. Dai, Y. Zhang, R. Dangol, Y. Zheng, B. Li, Y. Zong and Q. Yan, *Small*, 2018, **14**, 1703257.
8. Y. Wang, J. Wang, T. Xie, Q. Zhu, D. Zeng, R. Li, X. Zhang and S. Liu, *Appl. Surf. Sci.*, 2019, **485**, 506-512.
9. Y. Liu, S. Xu, X. Zheng, Y. Lu, D. Li and D. Jiang, *J. Colloid Interface Sci.*, 2022, **625**, 457-465.
10. J. Yan, L. Chen and X. Liang, *Sci. Bull.*, 2019, **64**, 158-165.
11. T. Zhang, X. Ren, S. Mo, W. Cao, C. Zhou, F. Ma, R. Chen, C. Zeng, L. Shi, T. Liu, H. Zhang and H. Ni, *J. Mater Sci. Technol.*, 2024, **199**, 66-74.
12. T. Zhang, X. Ren, W. Cao, H. Zou, X. Jiang, F. Ma, R. Chen, H. Qiao, Y. Zhang, H. Liu, H. Zhang and H. Ni, *J. Colloid Interface Sci.*, 2025, **679**, 569-577.
13. Q. Zhang, X. Zeng, Z. Zhang, C. Jin, Y. Cui and Y. Gao, *J. Colloid Interface Sci.*, 2024, **675**, 357-368.
14. D. Cao, J. Shao, Y. Cui, L. Zhang and D. Cheng, *Small*, 2023, **19**, 2301613.
15. C. Panda, P. W. Menezes, C. Walter, S. Yao, M. E. Miehlich, V. Gutkin, K. Meyer and M. Driess, *Angew. Chem. Int. Ed.*, 2017, **56**, 10506-10510.
16. J. Nai, X. Xu, Q. Xie, G. Lu, Y. Wang, D. Luan, X. Tao and X. W. Lou, *Adv. Mater*, 2021, **34**.
17. K. Guo, H. Li, J. Huang, Y. Wang, Y. Peng, S. Lu and C. Xu, *J. Energy Chem.*, 2021, **63**, 651-658.
18. C. Zhang, W. Xu, S. Li, X. Wang, Z. Guan, M. Zhang, J. Wu, X. Ma, M. Wu and Y. Qi, *Chem. Eng. J.,* 2023, **454**, 140291.
19. C. Xuan, Q. Xu, L. Han and B. Hou, *Chem. Eng. J.*, 2023, **464**.
20. K. Wan, J. Luo, X. Zhang, P. Subramanian and J. Fransaer, *Journal of Energy Chemistry*, 2021, **62**, 198-203.
21. J.-H. Park, H. J. Kwon, D. Y. Lee and S.-J. Suh, 2024, **20**, 2400046.
22. S. Niu, W.-J. Jiang, Z. Wei, T. Tang, J. Ma, J.-S. Hu and L.-J. Wan, *J. Am. Chem. Soc.*, 2019, **141**, 7005-7013.
23. J. Nai, Y. Lu, L. Yu, X. Wang and X. W. D. Lou, *Adv Mater.*, 2017, **29**.
24. H. Ren, L. Yu, L. Yang, Z.-H. Huang, F. Kang and R. Lv, *J. Energy Chem.*, 2021, **60**, 194-201.
25. J. Yu, W.-J. Li, G. Kao, C.-Y. Xu, R. Chen, Q. Liu, J. Liu, H. Zhang and J. Wang, *. Energy Chem.,* 2021, **60**, 111-120.
26. K. Xiao, L. Zhou, M. Shao and M. Wei, *J. Mater. Chem A*, 2018, **6**, 7585-7591.
27. A. Karmakar, A. V. Krishnan, R. Jayan, R. Madhu, M. M. Islam and S. Kundu, *Journal of Materials Chemistry A*, 2023, **11**, 10684-10698.
28. Y. Chen, Z. Ren, H. Fu, X. Zhang, G. Tian and H. Fu, *Small*, 2018, **14**, 1800763.